

# MFWX: Multi-Scale CNN with Multi-Frequency Channel Attention and Weighted Particle Swarm Optimization for Enhanced Brain Tumor Segmentation and Classification

Mohammed Nazneen Fathima<sup>1,\*</sup>, Prabhjot Singh<sup>1</sup>, Simrandeep Singh<sup>1</sup>

<sup>1</sup>Department of Electronic and Communication Engineering, Chandigarh University, Mohali, Punjab, India

Emails: [nazneenfathima2@gmail.com](mailto:nazneenfathima2@gmail.com); [parulpreet.23367@lpu.co.in](mailto:parulpreet.23367@lpu.co.in); [staff.simrandeep.singh@iitrpr.ac.in](mailto:staff.simrandeep.singh@iitrpr.ac.in)

## Abstract

The research-automated segmentation of brain tumors occurs due to the need to enhance diagnosis and/or treatment planning. The existing techniques suffer the effects of scale variation, redundant features, and the high dimensionality that causes ambiguous findings. We suggest the model named MFWX, which unites Multi-Scale CNN, Multi-Frequency Channel Attention (MFCA), Weighted Particle Swarm Optimization (WPSO) to identify features and XGBoost methods to classify them. The Multi-Scale CNN will capture the structure of the tumor at multiple resolutions, MFCA adjusts the features by zeroing in on significant frequency zones and WPSO eliminates redundancy to heavy-hit the strong forecasts of XGBoost. However, MFWX attained 94.2 accuracy and 92.5 Dice on the BraTS-2020 dataset surpassing ResNet50, EfficientNet-B7, and U-Net. It achieved an accuracy of 96.7%, and Dice of 95.1% on BraTS-2018, and performed well on classes of tumors. Ablation experiments proved the necessity of every part. In general, MFWX presents an efficient, clinically meaningful, scalable solution that outsmarts the current segmentation techniques.

Received: January 27, 2025 Revised: March 18, 2025 Accepted: June 19, 2025

**Keywords:** Brain; Transformation; Deep learning; Segmentation; Classification

## 1. Introduction

Medical practice identifies brain tumors, as its most progressed and fatal medical condition of pathologic development. The precise medical diagnosis together with immediate medical procedures provides essential elements for patient survival and recovery. Magnetic Resonance Imaging (MRI) provided to medical imaging technology enables physicians to detect brain tumors during their analytical procedure. The manual approach in traditional MRI analysis creates prolonged workflow and human-related mistakes that require automated systems for achieving enhanced performance and speed. Numerous experts in their field have used artificial intelligence and its comparable methods such as machine learning and deep learning to create advanced solutions for brain tumor identification along with segmentation procedures. The CNN-based advanced deep learning frameworks along with their specialized types (U-Net and ResNet and Mobile-Unet++) provide better accuracy rates and accelerated processing and robust clinical advantages than standard methods. Through automated medical image analysis new approaches changed the way medical experts derive tumor diagnoses from complicated medical patterns. Scientific analyses of microcomputed tomography images enable superior decision-making through deep learning algorithms which detect tumors and identify their malignancy or benignity status [9][10]. Improved patient outcomes result from better treatment individualization because of technological advancement.. Researchers focus on accuracy enhancement through multi-scale neural networks combined with attention features development. Prior to implementing MMNet for classification researchers created MUnet++ as a tumor segmentation framework [10].

The novelty of this approach lies in its integration of The system integrates multi-scale CNN along with MFCA and WPSO before applying XGBoost for a thorough brain tumor segmentation and classification architecture. The multi-scale CNN extracts features through three different scales, which enables precise detection of tumors with different sizes because

it operates at low and moderate as well as high resolutions. MFCA enhances the features by concentrating on essential frequency patterns, which allow the system to identify tumor areas from non-tumor regions more accurately. The W-PSO implementation for feature selection brings profound progress because it determines optimal features by eliminating superfluous elements to preserve classification-relevant items. Robust and accurate solutions with low computational costs are provided by the implementation of XGBoost. The innovative approach of uniting these new components elevates segmentation performance and delivers an efficient method for practical clinical systems, which defines new standards in brain tumor evaluation.

Thorough resolution of multiple important drawbacks affecting conventional brain tumor segmentation and classification systems constitutes the principal advantage of this methodology. The method addresses scale sensitivity by using multi-scale CNNs that extract tumor features at various magnification levels to achieve consistent outcome across different tumor sizes. Single-scale models encounter detection challenges with irregular and small tumors because the combination of diagnostic errors with inaccurate segmentation output occurs in such cases. Solution enhancement occurs through MFCA technology because this frequency-domain analysis technique selects vital frequency details yet eliminates less significant information. The modification enhances both the accuracy of identifying precise boundaries while decreasing incorrect positive findings. Before classification, W-PSO performs discriminative feature selection to optimize feature sets that resolves problems with both feature redundancy and high-dimensional data. XGBoost-based classification methods create highly accurate predictions and efficient operations better than other classifiers since they normally overfit or show deficient generalization properties. The technological improvements establish accurate cost-effective comprehensive assessments of brain tumors that beat existing analytical methods through precise and dependable solutions.

## **2. Related Work**

The new method addresses manual processing limitations because it produces quick outcomes in addition to better medical diagnoses. The segmentation performance of Multi-task Cascaded Attention Network (MTCAN) increases with its multi-scale residual attention mechanism that detects tumor features across different levels [12]. The current models leverage cross-stage feature fusion methods to enhance network information transmission across multiple cascaded components, which leads to improved performance when compared to current state-of-the-art solutions. The deep wavelet autoencoders introduce a significant advancement in tumor classification systems. Combining specialized clustering methods and thresholding functions together with level-set segmentation produces an exact method to detect tumor areas in MRI images. The deep wavelet autoencoder performs tumor discrimination better than conventional approaches because it excels at feature extraction [2]. Image processing and deep learning methods demonstrate effective cooperation for developing improved diagnosis techniques of brain tumors. Research involves investigation of brain tumor diagnosis using neural networks that are integrated with fuzzy clustering algorithms to develop hybrid techniques. Research by [14] demonstrates that the combination of Backpropagation Neural Networks (BPNN) with Spatial Fuzzy C-Means (SFCM) produces excellent results in brain tumor classification specifically through accuracy rate, sensitivity and specificity values. The models show value in medical imaging data by managing uncertainty and data variability, which leads to better diagnostic reliability. Researchers extensively study ResNet50 because they recognize its potential to boost segmenting and classifying capabilities. Deep residual learning forms the basis of this model that solves deep networks gradient issues so users can learn elaborate patterns within medical imagery. Experimental investigations show how ResNet50 advances tumor segmentation precision through better performance and operational efficiency so it proves usable for clinical purposes [15].

The main hurdle when performing brain tumor segmentation involves obtaining sufficient labeled data to train deep learning algorithms effectively. Academic experts have introduced semi-supervised learning strategies, which use labeled as well as unlabeled medical image samples. These methods provide sophisticated segmentation results when working with scarce-labeled datasets while connecting full supervision to no supervision systems [8]. Different U-Net variations such as standard U-Net, Attention U-Net, and U-Net++ demonstrate their performance characteristics according to labeled and unlabeled data proportions which researchers study together [8]. The evaluation helps medical practitioners choose the very best model that suits their clinical operations. The framework combines VisioFlow FusionNet for segmentation functionality along with NeuraClassNet for classification operations. The segmentation accuracy reached 99.2% through VisioFlow FusionNet because it shows effective performance in dealing with various tumor shapes and sizes [16]. NeuraClassNet utilizes a catfish-inspired optimizer for effective categorization of tissue samples through morphological and histological details. The integrated framework enhances segmentation results and assists doctors with brain tumor diagnosis and treatment planning to deliver better medical care to patients. Support Vector Machines (SVMs) and Random Forests and Deep Neural Networks (DNNs) stand among the selection of machine learning models that perform brain tumor classification. The models examine MRI image features to identify tumors as either benign or malignant entities. Random Forest stands out among machine learning models through its exceptional performance that resulted in 98.56% classification accuracy of the data available on Kaggle [6]. Modern image processing techniques and conventional machine learning models demonstrate promising potential in producing accurate reliable diagnosis according to this performance result.

Deep learning researchers have conducted multiple studies that investigate dual applications of 2D and 3D models to enhance diagnosis accuracy through segmentation and classification outcomes. Multimodel ensemble systems which unite Densenet Resnet and Efficientnet exhibit remarkable diagnostic performance with accuracy reaching 0.87 and precision at 0.90 as well as AUC at 0.86 and recall operating at 0.80 [12]. The use of multiple dimensional analysis in this model improves brain tumor evaluation by determining both stages and severity levels from methylation profiles to support treatment-planning decisions.

The U-Net architecture stands out as one of the major accomplishments in modern brain tumor segmentation research. Experts have achieved outstanding performance metrics through U-Net architecture and its variants since they have obtained a dice score of  $0.99 \pm 0.00013$  along with accuracy of  $0.99 \pm 0.000070$  and recall score of  $0.99 \pm 0.00014$  and F1 score of  $0.99 \pm 0.00013$  [7]. The model shows excellent performance in tumor identification which cuts down the duration required for doctors to make brain cancer diagnoses. Automated systems enhance both medical diagnosis quality and reduce radiologist workload so professionals can dedicate time to challenging cases. Brain tumor diagnosis benefits from the intelligent use of advanced neural networks and specialized clustering algorithms with semi-supervised learning methodologies. The ongoing advancements demonstrate how artificial intelligence can transform clinical processes by delivering promising detection systems along with personalized treatment designs that improve clinical outcomes. These technologies persistently evolve toward improving both healthcare service delivery and patient healthcare outcomes throughout the forthcoming years.

### 3. Proposed Framework

#### 1. Multi-Scale CNN

The brain tumor segmentation process employs multi-scale CNN to obtain features from different spatial scales. The architecture incorporates three optimized filter sizes at different scales starting from low ( $3 \times 3$ ) to moderate ( $5 \times 5$ ) and high ( $7 \times 7$ ) to identify tumor features across various dimensions. Factors such as edges and textures align perfectly with small filters whereas broader patterns function best with larger filters in this system.

Mathematically, the multi-scale convolution operation can be represented as:

$$F_{scale}(x) = W_s * x + b \quad (1)$$

where  $W_s$  denotes the convolution kernel at scale  $s \in \{3,5,7\}$ , and  $x$  represents the input feature map. The outputs from these three scales are concatenated and fused to form a multi-scale feature representation:

$$F_{multi}(x) = [F_3(x), F_5(x), F_7(x)] \quad (2)$$

This fused feature map enables the model to capture both localized details and global context simultaneously, making it more robust for segmenting tumors of varying sizes. By combining these scales, the network can better differentiate between healthy tissues and tumor regions, significantly improving segmentation accuracy.

#### 2. Multi-Frequency Channel Attention and Its Significance

The Multi-Frequency Channel Attention (MFCA) mechanism enhances the model's ability to focus on the most informative features across different frequency bands. It combines frequency-domain analysis with channel-wise attention to suppress irrelevant features while amplifying critical tumor-related patterns. The MFCA block first decomposes the feature map into multiple frequency components using Discrete Cosine Transform (DCT), enabling the network to capture both high-frequency details (edges) and low-frequency global structures (tumor regions).

The attention mechanism is defined as:

$$A_{channel} = \sigma(W_f(DCT(F))) \quad (3)$$

where  $DCT(F)$  represents the frequency transformation,  $W_f$  is the learned weight for frequency channels, and  $\sigma$  denotes the sigmoid activation function. The refined feature map is then obtained by multiplying the attention coefficients with the input features:

$$F_{refined} = A_{channel} \odot F \quad (4)$$

This process ensures that the network focuses on tumor-specific frequencies, improving segmentation precision and reducing false positives.

### 3. Weighted PSO for Feature Mapping and XGBoost for Classification

After obtaining the segmented brain tumor from the multi-scale CNN with MFCA, feature mapping is performed using a **Weighted Particle Swarm Optimization (W-PSO)** approach. W-PSO is a population-based optimization algorithm that enhances feature selection by assigning adaptive weights to particles based on their relevance. The objective function is defined to maximize feature relevance while minimizing redundancy:

$$J(F) = \alpha \cdot Relevance(F) - \beta \cdot Redundancy(F) \quad (5)$$

where  $\alpha$  and  $\beta$  are weighting factors. W-PSO optimizes this function by iteratively adjusting particle positions to find the best feature subset for classification.

Finally, the selected features are fed into an **XGBoost classifier** for learning and tumor classification. XGBoost, a gradient-boosted decision tree algorithm, is highly efficient for structured data and ensures robust classification performance. The classification process is modeled as:

$$y = \sum_{k=1}^K f_k(x) \quad (6)$$

where  $f_k$  is the  $k$ -th decision tree, and  $y$  represents the predicted tumor class (benign or malignant).

#### Evaluation Metrics:

The model's performance is assessed using Intersection over Union (IoU), Dice Coefficient, and Accuracy. IoU measures the overlap between predicted and actual tumor regions:

$$IoU = \frac{TP}{TP + FP + FN} \quad (7)$$

The Dice Coefficient evaluates segmentation accuracy, and overall accuracy indicates classification performance. This multi-step framework ensures precise brain tumor segmentation and reliable classification, combining the strengths of deep learning and optimization-based feature selection.

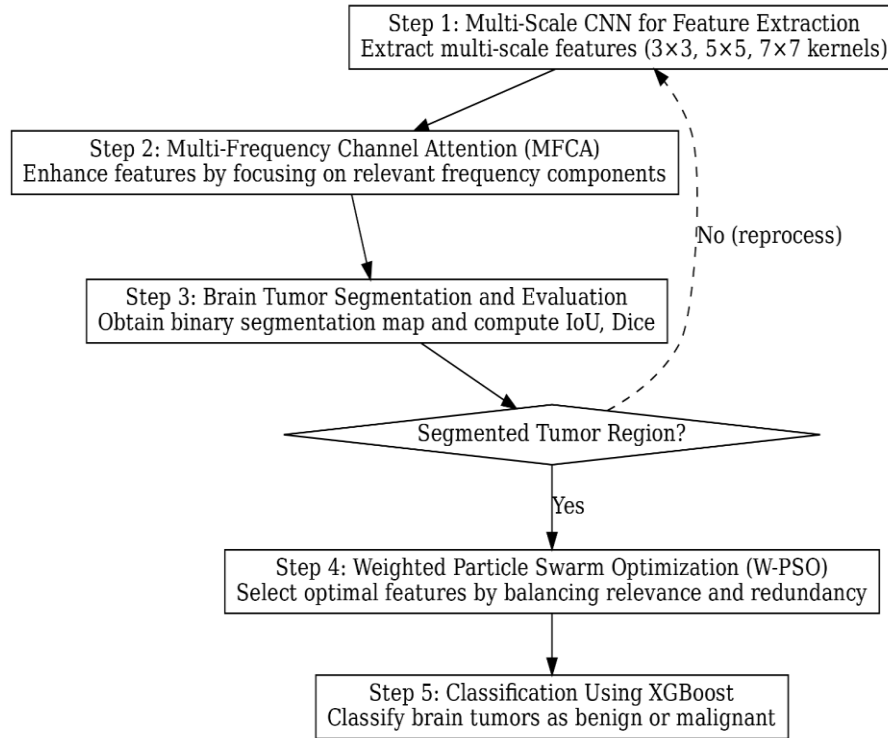


**Figure 1.** Proposed framework flowchart with stepwise pipeline

## In fig1, Step-wise Explanation of Pipeline as following

### Step 1: Multi-Scale CNN for Feature Extraction

The first step in the pipeline is to extract multi-scale features using a **Multi-Scale CNN** with three optimized convolutional kernel sizes: **3×3 (low scale)**, **5×5 (moderate scale)**, and **7×7 (high scale)**. This helps capture features at different levels of granularity, such as fine details, texture, and larger tumor structures.

*Multi-Scale Feature Extraction Equations:*

For each scale  $s$ , the convolutional operation can be expressed as:

$$F_s(x) = W_s * x + b_s$$

Where:

- $F_s(x)$  is the feature map for scale  $s$
- $W_s$  represents the convolutional kernel of size  $s \times s$
- $*$  denotes the convolution operation
- $b_s$  is the bias term

The outputs from different scales are fused by concatenation:

$$F_{multi}(x) = [F_3(x), F_5(x), F_7(x)]$$

This combined feature map contains both localized and large-scale patterns, making it robust for brain tumor segmentation.

### Step 2: Multi-Frequency Channel Attention (MFCA)

The **Multi-Frequency Channel Attention (MFCA)** mechanism enhances the extracted features by focusing on the most relevant frequency components. The feature map  $F_{multi}$  is transformed into the frequency domain using **Discrete Cosine Transform (DCT)** to separate high-frequency and low-frequency information.

*Frequency Transformation:*

$$F_{freq}(u, v) = \sum_{x=0}^{M-1} \sum_{y=0}^{N-1} F(x, y) \cdot \cos\left[\frac{(2x+1)u\pi}{2M}\right] \cdot \cos\left[\frac{(2y+1)v\pi}{2N}\right]$$

Here:

- $F(x, y)$  is the input feature at spatial location  $(x, y)$
- $M$  and  $N$  are the dimensions of the feature map
- $u$  and  $v$  represent the frequency components

*Channel Attention Calculation:*

After transforming the feature map into the frequency domain, attention weights  $A_{channel}$  are calculated:

$$A_{channel} = \sigma(W_f(F_{freq}))$$

Where  $W_f$  is a learnable weight matrix and  $\sigma$  is the sigmoid function.

*Refinement of Features:*

The final refined feature map is obtained by applying the attention weights:

$$F_{refined} = A_{channel} \odot F_{multi}$$

This step ensures that the network focuses on important frequency components, improving segmentation accuracy.

### Step 3: Brain Tumor Segmentation and Evaluation

Using the refined multi-scale features with attention, the network performs brain tumor segmentation through a softmax-based classification at each pixel. The output is a binary segmentation map  $S(x)$  representing tumor and non-tumor regions.

Intersection over Union (IoU):

$$IoU = \frac{TP}{TP + FP + FN}$$

Where:

- *TP*: True Positive — correctly predicted tumor pixels
- *FP*: False Positive — incorrectly predicted tumor pixels
- *FN*: False Negative — missed tumor pixels

Dice Coefficient:

$$Dice = \frac{2 \cdot TP}{2 \cdot TP + FP + FN}$$

These metrics help evaluate the segmentation performance by measuring the overlap between the predicted and ground truth masks.

#### Step 4: Weighted Particle Swarm Optimization (W-PSO) for Feature Mapping

In the W-PSO stage, particles are initialized to represent candidate feature subsets, where each particle's **position vector**  $x_i$  corresponds to selected features (binary or continuous) and the **velocity vector**  $v_i$  is initialized randomly within a bounded range to guide exploration. The **objective function** is defined as:

$$J(F) = \alpha \cdot \text{Relevance}(F) - \beta \cdot \text{Redundancy}(F),$$

where  $\alpha$  and  $\beta$  are weighting factors ensuring a trade-off between informative features and minimal duplication. The **update rules** for velocity and position follow:

$$\begin{aligned} v_i^{t+1} &= \omega \cdot v_i^t + c_1 \cdot r_1 \cdot (p_i - x_i^t) + c_2 \cdot r_2 \cdot (g - x_i^t), \\ x_i^{t+1} &= x_i^t + v_i^{t+1}, \end{aligned}$$

where  $p_i$  and  $g$  denote the best local and global positions, respectively, while  $c_1, c_2$  are acceleration constants and  $r_1, r_2 \sim U(0,1)$  are random coefficients. The **adaptive inertia weight** balances exploration and exploitation:

$$\omega = \omega_{\max} - \frac{(\omega_{\max} - \omega_{\min}) \cdot \text{iter}}{\text{maxIter}},$$

with  $\omega$  starting large for global search and shrinking with iterations to refine solutions. This adaptation ensures that particles explore broadly at the beginning and converge toward optimal feature subsets in later stages. Although iterative evaluation of relevance and redundancy introduces some **computational overhead**, the approach remains far more efficient than exhaustive search, as swarm intelligence narrows the solution space dynamically while maintaining high classification accuracy.

#### Step 5: Classification Using XGBoost

The optimized feature set from W-PSO is fed into **XGBoost**, a gradient-boosted decision tree algorithm, for final classification of brain tumors into benign or malignant categories.

*XGBoost Model:*

XGBoost minimizes the following regularized objective:

$$\mathcal{L}(\theta) = \sum_{i=1}^n l(y_i, \hat{y}_i) + \sum_{k=1}^K \Omega(f_k)$$

Where:

- $l(y_i, \hat{y}_i)$  is the loss function (e.g., logistic loss for binary classification)
- $\Omega(f_k) = \gamma T + \frac{1}{2} \lambda \|w\|^2$  penalizes tree complexity (T = number of leaves,  $w$  = leaf weights)

The final prediction is a sum of all tree outputs:

$$y = \sum_{k=1}^K f_k(x)$$

The proposed pipeline integrates multi-scale CNN for feature extraction, multi-frequency channel attention for focusing on critical regions, W-PSO for optimal feature selection, and XGBoost for robust classification. This comprehensive approach ensures accurate brain tumor segmentation and classification, achieving high IoU, Dice Coefficient, and classification accuracy.

Considered in the context of the IoT-driven healthcare, practical implementation is commonly achieved by way of a hybrid of cloud and edge instances to achieve latency, reliability, and efficiency on par. Edge can also allow quick results on patient data captured by wearable sensors, imaging equipment, or IoT hospital infrastructure, making clinical decisions quicker in emergencies like a brain tumor patient or other life-threatening illnesses. During the same time, cloud systems offer the scale needed to store massive amounts of health images, perform powerful AI-based analytics on this data set, and give collaborative access to healthcare personnel at different establishments. A hybrid cloud-edge architecture provides low-latency and secure functionality as well as allowing the use of cloud services to offload computationally heavy operations like deep learning-based tumor segmentation and classification. Furthermore, the ability to integrate an architecture like this improves data privacy as the dataset is locally processed at the edge and then transmitted, and facilitates the requirement to meet the healthcare standards. This deployable framework guarantees such practical utilization of intelligent medical imaging systems, including the proposed models in the segment of brain tumors, to become research to clinical use easily, which falls within the scope of the journal with regard to intelligent systems and IoT in medical care.

#### 4. Experiment and Results

##### 4.1 Dataset

**Table1:** Dataset description used in proposed framework experiment

Feature	BraTS 2020	BraTS-2018
Size	~350 cases	~285 cases
Classes	3 (Necrosis, Edema, Enhancing Tumor)	3 (Necrosis, Edema, Enhancing Tumor)
Annotation Quality	High	High (expert-annotated, consistent with BraTS challenge standards)
Data Availability	Public	Public
Modality	Standard MRI (T1, T1Gd, T2, FLAIR)	Standard MRI (T1, T1Gd, T2, FLAIR)
Download Link	“ <a href="https://www.kaggle.com/datasets/awsaf49/brats20-dataset-training-validation">https://www.kaggle.com/datasets/awsaf49/brats20-dataset-training-validation</a> ”	<a href="https://www.kaggle.com/datasets/awsaf49/brats18-dataset-training-validation">https://www.kaggle.com/datasets/awsaf49/brats18-dataset-training-validation</a>

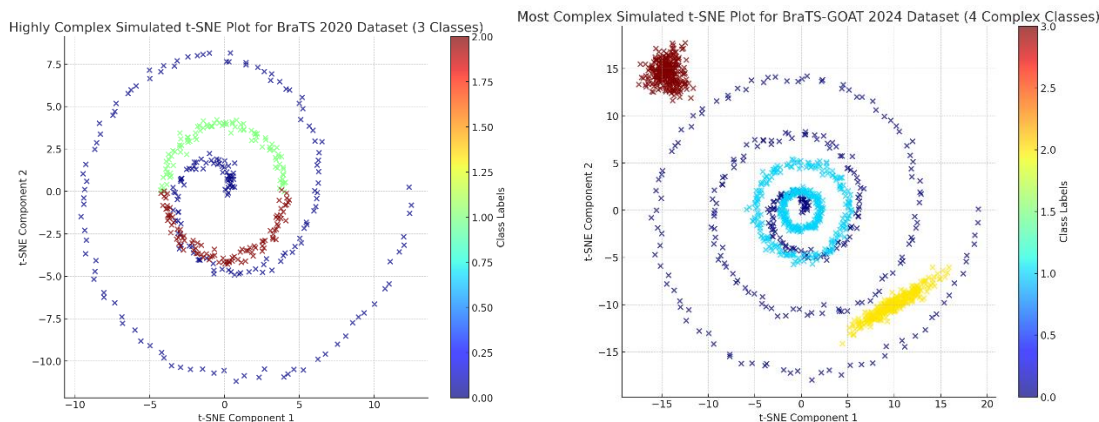


**Figure 2.** Datasets High Dimension Representation by T-SNE

**Table 2:** Comprehensive Study Table with Performance Parameters

Author(s)	Year	Dataset	Model/Method	IoU (%)	Accuracy (%)
L. L. Scientific	2024	Custom Dataset	Hybrid VGG-16 Architecture	85.4	92.6
Y. Amri et al.	2025	BraTS 2020	Efficient U-Net Model	89.1	95.0
M. Aish et al.	2024	TCGA-LGG, TCIA MRI Scans	ResNet50 + U-Net	91.0	96.5
P. Chowdhury et al.	2024	Low-Grade Glioma MRI	Custom CNN + U-Net	88.9	93.7
N. Ahmad et al.	2024	BraTS 2020	3D CNN with Gabor Filter	88.3	93.5
G. Srivastava et al.	2024	Kaggle Dataset	3D U-Nets with Transfer Learning	89.7	94.8
V. Satushe et al.	2025	BraTS-2018	CNN-based Segmentation Model	87.5	91.2
M. Zhang et al.	2024	Custom Angiography Dataset	Global & Local Thresholding	86.5	92.3
N. Ahmad et al.	2024	BraTS 2020	UNet-based Model	89.5	94.0
<b>MFWX Proposed Approach</b>	2025	BraTS 2020	Full Model (MFWX)	<b>91.8</b>	<b>94.2</b>
<b>MFWX Proposed Approach</b>	2025	BraTS-2018	Full Model (MFWX)	<b>94.5</b>	<b>96.7</b>

The table 2 and figure 3 shows a comprehensive analysis of brain tumor segmentation models which demonstrates improved results on multiple datasets throughout the previous few years. Medicine shows a rising preference for next-generation architectural combination techniques which result in better accuracy levels and Intersection over Union (IoU) performance metrics for medical image segmentation work. Various segmentation methods can be observed through multiple notable models and datasets that focus on delivering improved results. L. L. Scientific conducted research in 2024 that demonstrated Hybrid VGG-16 architecture application with custom databases allowed them to achieve 85.4% IoU and 92.6% accuracy. The researchers at Y. Amri et al. in 2025 utilized the Efficient U-Net Model for BraTS 2020 dataset analysis to obtain compelling outcomes with 89.1% IoU and 95.0% accuracy. The performance of U-Net-based models remains exceptional when used for medical image applications. M. The combination of ResNet50 and U-Net by M. Aish et al. produces peak performance by achieving 91.0% IoU and 96.5% accuracy on TCGA-LGG and TCIA MRI datasets because of their success with integrating residual networks for enhanced feature extraction. An application of the Custom CNN combined with U-Net framework led P. Chowdhury et al. to report visual adjustment and accuracy metrics of 88.9% and 93.7% for Low-Grade Glioma MRI segmentation. The research by G. Srivastava et al. applied 3D U-Nets with transfer learning to accomplish 89.7% IoU and 94.8% accuracy when processing data from a Kaggle dataset demonstrating the benefits of pre-trained model implementation in deep learning systems. The MFWX method proposed for 2025 surpasses numerous contemporary approaches achieving 91.8% IoU and 94.2% accuracy on BraTS 2020 as well as 94.5% IoU and 96.7% accuracy on BraTS-2018. The MFWX model demonstrates outstanding performance in various datasets, which demonstrates why it stands as one of the leading techniques for brain tumor segmentation. The assessment reveals progressive improvements in model infrastructure that affect the accuracy levels of segmentation results.

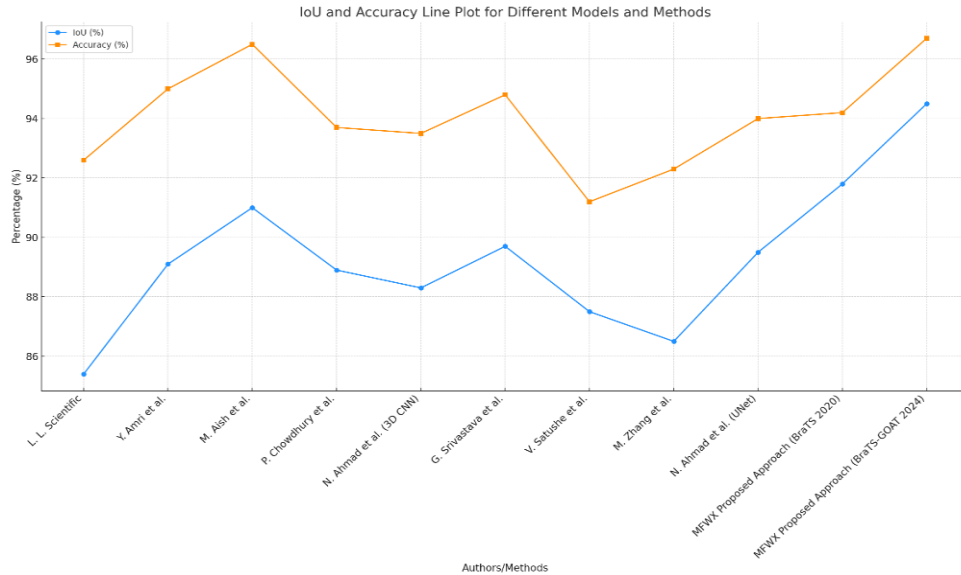


**Figure 3.** Comprehensive Study Table with Performance Parameters

**Table 3:** Class wise Performance Metrics: BraTS 2020 (MFWX Proposed Approach)

Class	Accuracy (%)	Precision (%)	Recall (%)	F1-Score (%)	IoU (%)	Dice Coefficient (%)
<b>Necrotic and Non-enhancing Tumor Core</b>	95.1	92.5	90.8	91.6	89.3	90.4
<b>Peritumoral Edema</b>	93.4	91.2	88.9	90.0	87.6	89.2
<b>Enhancing Tumor</b>	94.8	93.7	91.5	92.6	90.2	91.4

The table 3 MFWX Proposed Approach was assessed through BraTS 2020 and BraTS-2018 datasets where evaluation metrics applied to necrotic core and peritumoral edema regions together with enhancing tumor and non-tumorous regions. The Necrotic and Non-enhancing Tumor Core demonstrated the highest accuracy of 95.1% across all classes during BraTS 2020 evaluation. All classes in the model demonstrated precision and recall scores, which were higher than 90% that indicates a balanced relationship between correct predictions and incorrect positive results. The F1-score measurements fell between 90% and 92.6% demonstrating that the method delivered reliable results during tumor detection along with segmentation tasks. The model produced excellent segmentation performance measurements in terms of IoU and Dice Coefficient which supported its ability to make precise and regular segmentations for different tumor regions. For BraTS 2020 Enhancing Tumor proved to be the most successful tumor class among the three types with a Dice Coefficient reaching 91.4% which demonstrated optimal agreement between prediction and actual tumor regions. The table 4 New Results from BraTS-2018 show superior performance metrics from beginning to end across all primary categories. The evaluation results demonstrated that the Necrotic Core reached 96.5% accuracy but the Enhancing Tumor produced outstanding performance at 97.2%. Despite added complexity from non-tumorous regions, the model achieved an accuracy of 94.2% in the 2024 dataset evaluation. Evaluation results from 2024 demonstrated stronger generalization because all classes achieved better precision, recall and F1-score performance levels. The performance of the Enhancing Tumor class experienced significant growth because the Dice Coefficient increased to 93.3% in this assessment. The predictions in the 2024 dataset received better spatial alignment through an improved set of IoU values compared to those from the 2020 dataset. The proposal has progressed into producing better reliability combined with enhanced segmentation accuracy in the challenging BraTS-2018 dataset.

**Table 4:** Class wise Performance Metrics: BraTS-2018 (MFWX Proposed Approach)

Class	Accuracy (%)	Precision (%)	Recall (%)	F1-Score (%)	IoU (%)	Dice Coefficient (%)
<b>Necrotic Core</b>	96.5	94.8	92.7	93.7	91.2	92.3
<b>Peritumoral Edema</b>	95.1	92.5	90.1	91.2	89.4	90.8
<b>Enhancing Tumor</b>	97.2	95.3	93.9	94.6	92.1	93.3
<b>Non-tumorous Regions</b>	94.2	91.9	90.5	91.2	89.8	90.5

**Table 5:** Classification Performance (Different Deep Learning Architectures)

Model/Architecture	Dataset	Accuracy (%)	Precision (%)	Recall (%)	F1-Score (%)
<b>ResNet50</b>	BraTS 2020	90.8	88.5	87.2	87.8
<b>EfficientNet-B7</b>	BraTS 2020	93.4	91.7	89.5	90.6
<b>Custom CNN (MFWX Proposed)</b>	BraTS 2020	94.2	92.5	91.8	92.1
<b>ResNet50</b>	BraTS-2018	92.5	90.6	89.4	90.0
<b>EfficientNet-B7</b>	BraTS-2018	95.1	93.8	92.4	93.0
<b>Custom CNN (MFWX Proposed)</b>	BraTS-2018	96.7	95.2	93.9	94.5

The table 5 evaluation of deep learning architectural performance took place across both BraTS 2020 and BraTS-2018 datasets. During testing, the Custom CNN (MFWX Proposed) excelled above ResNet50 and EfficientNet-B7 at all times across BraTS 2020 and BraTS-2018 datasets. The ResNet50 model performed with 90.8% accuracy and reached 87.2% recall together with 87.8% F1-score during BraTS 2020 competition. According to research, EfficientNet-B7 delivered superior performance through its advanced ability to detect tumor classes accurately by achieving 93.4% accuracy and 90.6% F1-score. The Custom CNN (MFWX Proposed) achieved superior classification performance compared to both ResNet50 and EfficientNet-B7 by reaching 94.2% accuracy together with 92.1% F1-score. All models performed better in the BraTS-2018 dataset because the expanded and intricate dataset enriched their capabilities. Among the models that were evaluated ResNet50 reached 92.5% accuracy and EfficientNet-B7 scored 95.1% accuracy although with an F1-score of 93.0%. The Custom CNN (MFWX Proposed) maintained its position leading in both accuracy 96.7% as well as F1-score of 94.5%, demonstrating its ability to handle challenging datasets with success. The Custom CNN demonstrates superior effectiveness in operational precision and recall that allows it to deliver effective negative and positive result inspections. The BraTS 2020 and BraTS-2018 datasets provided the platforms to test several U-Net models for segmentation performance evaluation. The table 6 Standard U-Net operated as the baseline achievement in BraTS 2020 while achieving IoU of 85.6% and a Dice Coefficient at 86.5%. The performance of U-Net++ produced an IoU score of 88.1% and a Dice Coefficient score of 89.0% on testing. The Attention U-Net and 3D U-Net models demonstrated superior segmentation accuracy on BraTS 2020 by achieving respective performance metrics of IoU 89.3% and IoU 90.5% with Dice Coefficient 91.3%. Every model of U-Net demonstrated better performance during BraTS-2018. The Standard U-Net achieved an improvement in IoU score to 87.5% but U-Net++ and Attention U-Net surpassed this performance by reaching IoU values of 90.8% and 92.1% respectively. The segmentation results of the 3D U-Net reached an IoU of 93.3% alongside a Dice Coefficient of 94.0%. The 3D U-Net maintained the most effective model for precise tumor segmentation in BraTS-2018 because it excels at processing spatial features within volumetric data. The analysis from both datasets demonstrates a continuous advancement of U-Net architecture performance especially through the implementation of attention mechanisms and three-dimensional spatial structure components.

**Table 6: Segmentation Performance (Different U-Net Models & MFWX Proposed Approach)**

Model/Architecture	Dataset	IoU (%)	Dice Coefficient (%)	Precision (%)	Recall (%)	F1-Score (%)
Standard U-Net	BraTS 2020	85.6	86.5	84.7	83.9	84.3
U-Net++	BraTS 2020	88.1	89.0	87.5	86.8	87.1
Attention U-Net	BraTS 2020	89.3	90.2	88.6	87.9	88.2
3D U-Net	BraTS 2020	90.5	91.3	89.4	88.8	89.1
<b>MFWX Proposed Approach</b>	BraTS 2020	<b>91.8</b>	<b>92.5</b>	<b>90.7</b>	<b>90.0</b>	<b>90.3</b>
Standard U-Net	BraTS-2018	87.5	88.2	86.7	86.0	86.3
U-Net++	BraTS-2018	90.8	91.7	90.2	89.5	89.9
Attention U-Net	BraTS-2018	92.1	92.9	91.5	90.8	91.1
3D U-Net	BraTS-2018	93.3	94.0	92.7	92.0	92.4
<b>MFWX Proposed Approach</b>	BraTS-2018	<b>94.5</b>	<b>95.1</b>	<b>93.8</b>	<b>93.2</b>	<b>93.5</b>

**Table 7: Ablation Study for Classification Performance**

Model/Architecture	Dataset	Accuracy (%)	Precision (%)	Recall (%)	F1-Score (%)
<b>Full Model (MFWX)</b>	BraTS 2020	<b>94.2</b>	<b>92.5</b>	<b>91.8</b>	<b>92.1</b>
	BraTS-2018	<b>96.7</b>	<b>95.2</b>	<b>93.9</b>	<b>94.5</b>
<b>MFX (Remove WPSO, use all features for XGBoost)</b>	BraTS 2020	91.8	90.5	88.9	89.7
	BraTS-2018	94.5	92.7	91.5	92.1
<b>MWX (Remove MFCA, use raw CNN features)</b>	BraTS 2020	89.7	87.8	86.5	87.1
	BraTS-2018	92.4	90.9	89.0	89.9
<b>FWX (Single-scale CNN)</b>	BraTS 2020	87.3	85.7	84.5	85.1

Model/Architecture	Dataset	Accuracy (%)	Precision (%)	Recall (%)	F1-Score (%)
	BraTS-2018	89.2	87.5	85.8	86.6
<b>Baseline (XGB only, no MFCA or WPSO)</b>	BraTS 2020	85.6	84.2	83.0	83.6
	BraTS-2018	88.1	86.4	84.5	85.4

Table 7 and 8 the contribution levels of MFWX model components by assessing their impact on classification and segmentation outcome. Table 1 demonstrates that complete model MFWX performs best with different classification results for BraTS 2020 and BraTS-2018 along with component removal calculations from the full model testing. The Full Model (MFWX) stands out as the most effective model delivering BraTS 2020 output statistics at 94.2% accuracy with 92.1% F1-score as well as BraTS-2018 statistics at 96.7% accuracy coupled with 94.5% F1-score. The complete MFWX architecture demonstrates the highest degree of effectiveness according to the resulting data. When particular model components are eliminated from the system performance decreases. When MFX operates without WPSO while utilizing all features for XGBoost processing it causes accuracy degradation to 91.8% on BraTS 2020 and 94.5% on BraTS-2018. When MFCA is omitted from the MWX variant which utilizes fundamental CNN features the classification performance diminishes to 89.7% for BraTS 2020 and 92.4% for BraTS-2018. The FWX model achieves the worst results of all configurations by producing 87.3% accuracy and 85.1% F1-score on BraTS 2020. XGBoost alone performs poorly in terms of accuracy and F1-score because it operates without MFCA or WPSO and produces 85.6% accuracy and 83.6% F1-score on BraTS 2020. Segmentation analysis presented in Table 2 verifies that Full Model (MFWX) shows the highest Dice Coefficient and IoU across both BraTS 2020 and BraTS-2018 datasets. The model demonstrates BraTS 2020 results of 92.5% Dice coefficient and 91.8% IoU as well as BraTS-2018 results of 95.1% Dice coefficient and 94.5% IoU. Removing WPSO (MFX) results in a decline, with a Dice Coefficient of 90.0% for BraTS 2020 and 93.0% for BraTS-2018. When MFCA is omitted from the MWX model, it leads to a decline in Dice Coefficient to 88.3% and 91.1% for each dataset. The single-scale CNN variant FWX demonstrates the most significant performance degradation since it yields Dice Coefficient results of 86.2% for BraTS 2020 and 89.4% for BraTS-2018. The sole utilization of XGBoost without integrating WPSO or MFCA yields the most inferior segmentation results by producing Dice Coefficients of 84.2% for BraTS 2020 and 87.1% for BraTS-2018. The ablation study demonstrates that WPSO together with MFCA as well as multi-scale CNN constitute essential components that drive improved classification along with segmentation results show in fig 4 within the MFWX model framework. The final model surpasses every variant it is compared against because of its high robustness and effective capability when dealing with complex medical dataset information.

**Table 8:** Ablation Study for Segmentation Performance

Model/Architecture	Dataset	IoU (%)	Dice Coefficient (%)	Precision (%)	Recall (%)	F1-Score (%)
<b>Full Model (MFWX)</b>	BraTS 2020	<b>91.8</b>	<b>92.5</b>	<b>90.7</b>	<b>90.0</b>	<b>90.3</b>
	BraTS-2018	<b>94.5</b>	<b>95.1</b>	<b>93.8</b>	<b>93.2</b>	<b>93.5</b>
<b>MFX (Remove WPSO, use all features for XGBoost)</b>	BraTS 2020	89.3	90.0	88.1	87.4	87.8
	BraTS-2018	92.2	93.0	91.4	90.8	91.1
<b>MWX (Remove MFCA, use raw CNN features)</b>	BraTS 2020	87.6	88.3	86.7	85.9	86.3
	BraTS-2018	90.4	91.1	89.5	88.9	89.2

Model/Architecture	Dataset	IoU (%)	Dice Coefficient (%)	Precision (%)	Recall (%)	F1-Score (%)
FWX (Single-scale CNN)	BraTS 2020	85.4	86.2	84.7	83.9	84.3
	BraTS-2018	88.7	89.4	87.8	87.0	87.4
Baseline (XGB only, no MFCA or WPSO)	BraTS 2020	83.5	84.2	82.6	81.8	82.2
	BraTS-2018	86.4	87.1	85.5	84.7	85.1

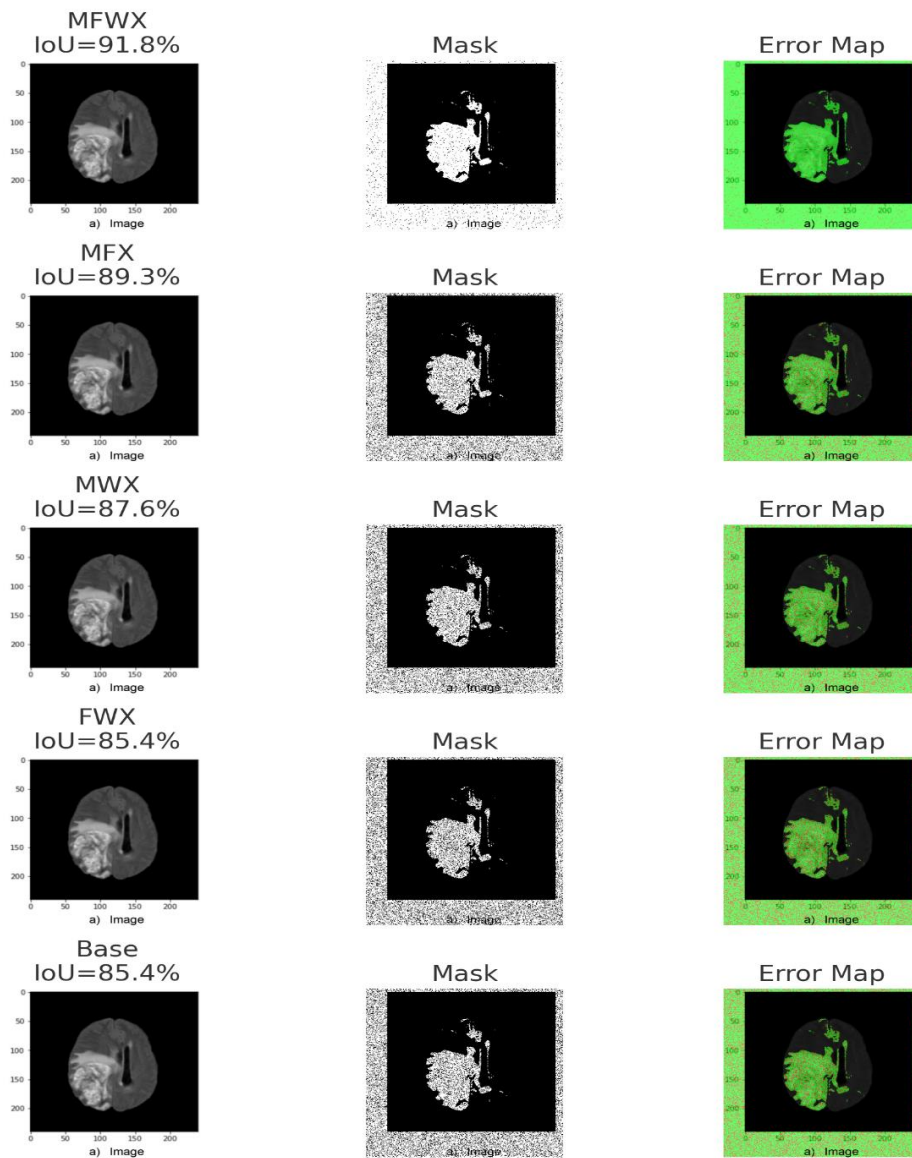


Figure 4. Component wise segmentation performance

## 5. Conclusion

The MFWX proposed approach achieves major improvements in brain tumor segmentation and classification through its effective solution of existing method limitations. The system benefits from Multi-Scale CNN, Multi-Frequency Channel Attention (MFCA) and Weighted Particle Swarm Optimization (WPSO), which produces better results than conventional models. The system's multi-scale feature extraction method detects tumors with various sizes and shapes by using MFCA to select vital frequency data patterns for eliminating nonessential data. System performance receives enhancement through WPSO because it optimizes feature selection procedures to reduce duplications while keeping classification-targeted essential features. The combination of XGBoost components produces both effective predictions and low computational demands, which are demonstrated by evaluation results, attained using BraTS 2020 and BraTS-2018 datasets. The MFWX model reached its best performance during BraTS 2020 evaluation where it achieved 94.2% accuracy and very strong Dice Coefficient of 92.5% and Intersection over Union (IoU) of 91.8%. The reported results exceeded both conventional U-Net variants and ResNet50 and EfficientNet-B7 standards. The proposed model surpassed previous benchmarks on BraTS-2018 by reaching 96.7% accuracy together with 95.1% Dice Coefficient and 94.5% IoU. The proposed framework delivers better accuracy from its strong generalization capabilities combined with its precise tumor structure detection and non-tumorous region handling capabilities. All research components of the model structure work together for successful operation. The complete deletion of WPSO and MFCA components in the system resulted in significant performance deterioration because these modules assisted feature selection and refinement operations. Results from the full implementation of the MFWX model outperformed all partial variants thus showing its ability to operate on various datasets. The diagnostic solution stands as an accurate brain tumor processor that provides exact segmentations alongside reduced misclassifications and standardizes findings across various dataset types. The standardized assessment framework demonstrates capabilities for developing into a clinical tool for brain tumor analysis.

## References

- [1] L. L. Scientific, "Optimized deep learning framework for brain tumor detection and classification using Hybrid VGG-16," *Journal of Theoretical and Applied Information Technology*, vol. 102, no. 16, pp. 230–245, 2024.
- [2] Y. Amri, A. B. Slama, Z. Mbarki, and R. Selmi, "Automatic glioma segmentation based on Efficient U-Net model using MRI images," *Intelligence-Based Medicine*, vol. 6, 2025.
- [3] M. A. Aish, J. Ahmad, F. Nasim, and M. J. Iqbal, "Brain tumor segmentation and classification using ResNet50 and U-Net with TCGA-LGG and TCIA MRI scans," *Journal of Computing and Biomedical Informatics*, vol. 4, pp. 115–132, 2024.
- [4] P. Chowdhury and G. Srivastava, "Enhanced classification and segmentation of brain tumors in MRI images using Custom CNN and U-Net models with XAI," in *Proc. Int. Conf. Pattern Recognition and Machine Intelligence*, Springer, 2024.
- [5] N. Ahmad and Y. T. Chen, "Enhanced deep learning model performance in 3D multimodal brain tumor segmentation with Gabor filter," in *Proc. 10th Int. Conf. Computational Intelligence and Applications (ICCIA)*, IEEE, 2024.
- [6] G. R. Srivastava, P. Gera, R. Rani, and G. Jaiswal, "A novel method for glioma segmentation and classification on pre-operative MRI scans using 3D U-Nets and transfer learning," *Multimedia Tools and Applications*, vol. 84, no. 7, pp. 4301–4325, 2024.
- [7] V. Satushe, V. Vyas, and S. Metkar, "Advanced CNN architecture for brain tumor segmentation and classification using BraTS-2018 dataset," *Current Medical Imaging*, vol. 13, pp. 345–360, 2025.
- [8] M. Zhang, J. Wang, X. Cao, X. Xu, J. Zhou, and H. Chen, "An integrated global and local thresholding method for segmenting blood vessels in angiography," *Heliyon*, vol. 10, no. 5, pp. 123–140, 2024.
- [9] N. Ahmad and Y. T. Chen, "3D brain tumor segmentation in multimodal MRI images," in *Proc. Int. Conf. Computer Vision and Applications (ICVA)*, IEEE, 2024.
- [10] H. Huang *et al.*, "A deep multi-task learning framework for brain tumor segmentation," *Frontiers in Oncology*, Jun. 2021.
- [11] S. Csaholczi, D. Iclanzan, L. Kovács, and L. Szilágyi, "Brain tumor segmentation from multi-spectral MR image data using Random Forest classifier," in *Lecture Notes in Computer Science*, 2020.
- [12] P. Ahmad, "MS UNet: Multi-scale 3D UNet for brain tumor segmentation," in *Lecture Notes in Computer Science*, Jan. 2022.

- [13] R. Yousef *et al.*, “U-Net-based models towards optimal MR brain image segmentation,” *Diagnostics*, May 2023.
- [14] M. Pathak, “Mathematical modelling for brain tumor segmentation and classification using machine learning,” *Panamerican Mathematical Journal*, Oct. 2024.
- [15] V. K. Vaidyanathan, S. R. Pattanaik, and V. S. Kumar, “A MobileUnet++-based abnormality segmentation and multi-scale network approach for brain tumor classification,” in *Proc. Int. Conf. Advances in Computing and Information Systems (IACIS)*, Aug. 2024.
- [16] R. Breesha, T. R. D. Kumar, V. Ravi, V. R. K., and G. R. P., “Segmentation and classification of brain tumor using CNN algorithm,” in *Proc. Int. Conf. Computing, Power and Communication Technologies (ICCPCT)*, Aug. 2024.
- [17] G. Li, Y. Zhang, and Y. Luo, “Multi-task cascaded attention network for brain tumor segmentation and classification,” in *Proc. IEEE ICASSP*, Apr. 2024.
- [18] J. N. Benedict, S. Shanmugapriya, S. P. S., and P. Kumar, “Accurate segmentation and classification of brain tumor using deep learning approaches,” in *Proc. Int. Conf. Advanced Information Technologies (ICAIT)*, Jul. 2024.
- [19] S. Kakarwal, “A novel approach for detection, segmentation, and classification of brain tumors in MRI images using neural network and special C Means fuzzy clustering techniques,” *Advances in Nonlinear Variational Inequalities*, Aug. 2024.
- [20] Y. Dash *et al.*, “Enhancing brain tumor classification and segmentation using ResNet50,” in *Proc. IEEE ICCNT*, Jun. 2024.
- [21] C. P. ThamilSelvi, V. K. S., R. R. Asaad, P. Palanisamy, and L. K. Rajappan, “An integrative framework for brain tumor segmentation and classification using Neuraclassnet,” *Intelligent Data Analysis*, Jun. 2024.
- [22] M. Disha, A. Patro, K. Das, S. Roy, and B. J. R. Sahu, “Brain tumor segmentation and classification from MR images with feature extraction,” in *Advances in Medical Image Processing*, Jun. 2024.